



Mechanism of boron removal from Si–Al melt by Ar–H₂ gas mixtures

Jing-wei LI, Xiao-long BAI, Bo-yuan BAN, Qiu-xiang HE, Jian CHEN

Key Laboratory of Novel Thin Film Solar Cells, Institute of Applied Technology,
Chinese Academy of Science, Hefei 230031, China

Received 9 October 2015; accepted 11 April 2016

Abstract: A new method about purification of metallurgical grade silicon (MG-Si) by a combination of Si–Al solvent refining and gas blowing treatment was proposed. The morphologies and transformation of impurity phases, especially for boron and iron in Si–Al melt were investigated during Ar–H₂ gas blowing treatment. The mechanism of boron removal was discussed. The results indicate that gas blowing can refine grain size and increase nucleation of the primary Si. Boron can be effectively removed from MG-Si using the Ar–H₂ gas blowing technique during the Si–Al solvent refining. Compared with the sample without gas blowing, the removal efficiency of boron increases from 45.83% to 74.73% after 2.5 h gas blowing. The main impurity phases containing boron are in the form of TiB₂, AlB₂ and VB compounds and iron-containing one is in the form of β -Al₃FeSi intermetallic compound. Part of boron combines [H] to transform into gas B_xH_y (BH, BH₂) and diffuses towards the surface of the melt and is volatilized by Ar–H₂ gas blowing treatment under electromagnetic stirring.

Key words: metallurgical grade silicon; Si–Al melt; gas blowing; boron removal

1 Introduction

The removal of boron in metallurgical grade silicon (MG-Si) is one of the most crucial tasks for upgrading to the photovoltaic silicon feedstock [1]. Several processes, such as slag refining [2], plasma treatment [3], and solvent refining [4] have been reported for this purpose.

Impurities in the MG-Si shorten the lifetime of excited carries in Si-based solar cells and disturb electric generation [5]. Hence, their removal from Si is an important issue on Si solar cells fabrication. Solvent refining is a purification process that relies on preferential segregation of impurities to a liquid, in which high purity solid silicon crystals grew from. Al as an effective solvent, has been investigated by many researchers [4,6,7]. During the Al–Si solvent refining process, the impurity elements are rejected into the Al–Si eutectic melt and the segregation behaviour of the impurity elements determines the removal efficiency. In order to improve the removal efficiency of boron from Al–Si melt, many works emphasized on thermodynamic evaluation, separation of the refined Si and kinetic

factors of the Al–Si solvent refining process. The segregation coefficients of boron and phosphorus between solid Si and Al–Si melt have been calculated by many researchers with different methods [4,8,9]. Some external fields, such as electromagnetic force [10] and super gravity [11], have been applied to separating the primary Si from the Al–Si melt. Besides, the kinetic factors [12,13], such as cooling rate, Si proportion, and refining temperature, or the introduction of other additives [14,15] have been investigated to improve the purity of the refined Si. Gas blowing treatment [16,17] is an effective way to remove boron from MG-Si, but with the disadvantage of high temperature, essential hydrogen water vapour, small contact area, and closed system. However, as for the effect of gas blowing, especially for the H₂ without water vapor, the boron removal at low temperatures during Al–Si solvent refining process has not been investigated.

In the present work, a new method of solvent refining has been proposed to obtain higher removal efficiency of boron during Al–Si solvent refining. The efficiency of boron removal is evaluated by introducing into Ar–H₂ gas mixtures into the Al–Si melt and

Foundation item: Projects (51404231, 51474201) supported by the National Natural Science Foundation of China; Project (1508085QE81) supported by Anhui Provincial Natural Science Foundation, China; Project (2014M561846) supported by China Postdoctoral Science Foundation; Project (2012065) supported by 100 Talent Program of Chinese Academy of Sciences

Corresponding author: Jian CHEN; Tel: +86-551-65592171; E-mail: jchen@ipp.ac.cn

DOI: 10.1016/S1003-6326(16)64435-7

compared with that without Ar–H₂ gas mixtures. The distribution of boron and transformation of impurity phases, especially TiB₂, AlB₂ and VB, etc., in the Al–Si alloy after the gas blowing treatment were investigated. Mechanism of boron removal was discussed based on the experimental results.

2 Experimental

Figure 1 shows a schematic drawing of the 25 kW induction furnace used in this work. 6N pure silicon (99.9999%) was first alloyed with analytical reagent pure boron powder to about 186×10^{-6} in a high-purity graphite crucible. 90 g boron doped Si and 210 g high purity aluminum were then put into a high-purity alumina crucible with an inner diameter of 55 mm and height of 100 mm. After the crucible was positioned into the medium frequency induction furnace, the system was then filled with Ar to protect graphite crucible. Raising the temperature to melt Al–Si mixture, then a H₂–Ar mixture was blown into the melt through a 5 mm inner diameter quartz tube. The gas blowing rate was controlled at 3 L/min and the gas ratio of H₂ to Ar was 1:1 for H₂–Ar mixture. The temperature profiles of the samples were carefully controlled by adjusting the induction power of the furnace. After the gas blowing treatment, the Al–Si melt was sampled into the cold crucible from the melt by a quartz tube every 30 min and the sample was solidified rapidly at room temperature. The duration of each experiment within gas blowing was from 0 to 330 min. Then, the power was cut off and the Al–Si melt was slowly solidified to the room temperature in the furnace. Lastly, the solidified Al–Si alloy samples (containing the rapidly and slowly solidified samples) were put into acid solution to remove Al to obtain refined Si. The acid solutions were HCl solution and the duration of acid leaching was 48 h at 353 K. Then, the impurity concentrations in the refined Si were examined by inductively coupled plasma optical emission spectroscopy (ICP-OES), and the

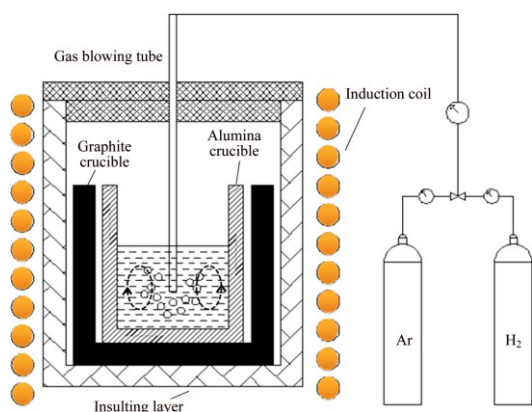


Fig. 1 Schematic drawing of 25 kW induction furnace

morphologies were analyzed by scanning electron microscope (SEM).

3 Results and discussion

3.1 Morphology of Al–Si alloy

Figure 2 shows the microstructures of the solidified Al–Si alloy with different Ar–H₂ treatment time and cooling rates. As can be seen from Figs. 2(a) and (b), the Al–Si melt was sampled into the cold crucible directly with different gas blowing treatment time. The primary silicon crystals are distributed uniformly in the alloy. The average length of the primary Si crystals in the alloy is about 500 μm without Ar–H₂ blowing. After 3.5 h

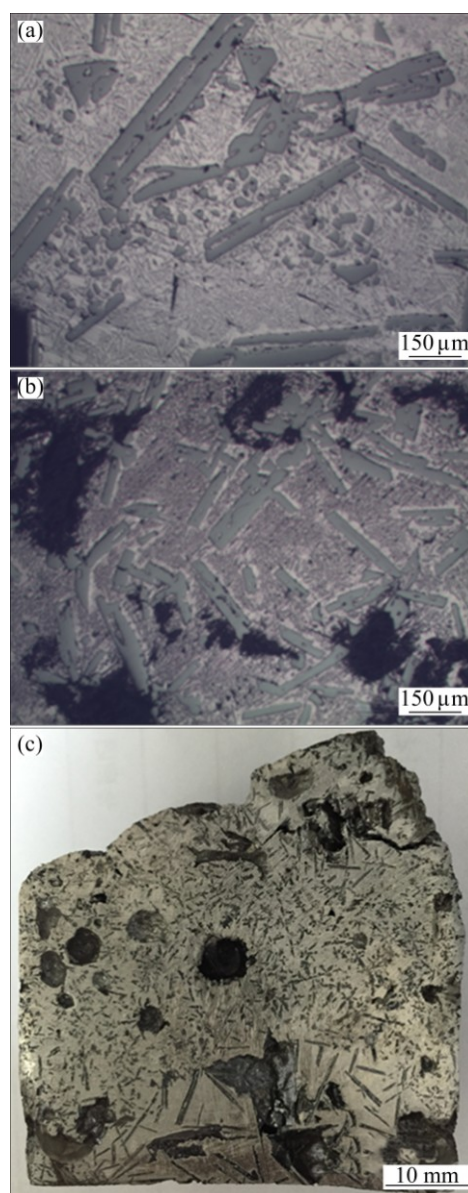


Fig. 2 Microstructures of Al–30%Si: (a) Without Ar–H₂ blowing, rapidly cooling in cold crucible; (b) 3.5 h Ar–H₂ blowing, rapidly cooling in cold crucible; (c) 5.5 h Ar–H₂ blowing, slowly cooling in furnace

Ar–H₂ blowing treatment, the average length of the primary Si in the alloy is 300 μm, which is shorter than that without gas blowing.

As for the reason, the Ar–H₂ mixture was directly blown into the melt without preheating, which lowered the local melt temperature and increased nucleation of the primary Si. Moreover, the shear force produced by the Ar–H₂ bubbles could break the long primary Si particles. Based on the microstructure change of the primary Si phases, it can be concluded that the Ar–H₂ blowing can refine the grain size and increase the nucleation of the primary Si phases.

In Fig. 2(c), many holes uniformly distribute in the Al–30%Si alloy within 5.5 h Ar–H₂ blowing after furnace cooling. Obvious stratification appears. Large needle-like primary Si crystals are agglomerated at the bottom of the ingot and the average length of primary silicon is more than 5 mm. The distributions of primary silicon crystals are different from the samples, as shown in Figs. 2(a) and (b) because of the difference of cooling rates. In Figs. 2(a) and (b), the Al–Si melt was directly sampled into the cold crucible with rapid cooling rate. And the primary silicon crystals are small and uniformly distribute in the sample. However, in Fig. 2(c), the Al–Si melts were solidified slowly in the induction furnace when the power was cut off. This phenomenon is similar to the work by YOSHIKAWA and MORITA [18].

3.2 Removal efficiency of boron by gas blowing

Figure 3 shows the relationship between gas blowing time and removal efficiency of boron. The Al–Si melt was sampled into the cold crucible directly with different gas blowing treatment time. As can be seen from Fig. 3, the removal efficiency of boron becomes large with increasing of blowing time. When the gas blowing time is zero, which is without gas blowing, the mass fraction of boron in the refined Si is 101×10^{-6} , and the removal efficiency of boron is 45.83%. As for Al–Si solvent refining, YOSHIKAWA et al [6,19] and LI et al [11] have investigated the removal efficiency of boron in the refined Si and both of them have high removal efficiency of boron, more than 90%. However, because of the different cooling rates of Al–Si melt, in this part, the Al–Si melt after gas blowing was directly sampled into the cold crucible from the furnace with high cooling rate. The boron removal rate is controlled by kinetic factor, such as cooling rate [13]. For YOSHIKAWA et al [6,19], the sample was pulled down to the furnace with low cooling rate in the range of 5–10 K/min. Therefore, the removal efficiency of boron in this experiment was less than that in the previous literature. When the blowing time increased from 0.5 to 2.5 h, the removal efficiency of boron was improved from 46.05% to 74.73%. After 2.5 h blowing time

treatment, the mass fraction of boron decreases from 186.46×10^{-6} to 47.12×10^{-6} . Compared with the sample without gas blowing, the removal efficiency increases by 28.9% after 2.5 h gas blowing. These results demonstrated that blowing with Ar–H₂ mixture in the Al–Si melt can improve the removal efficiency of boron during solvent refining.

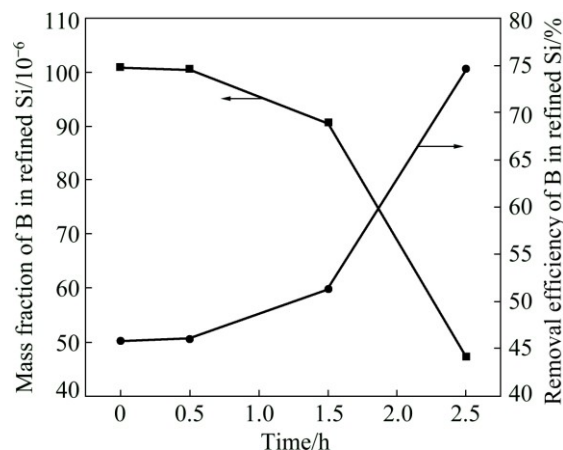


Fig. 3 Dependence of removal efficiency of boron on gas blowing time

3.3 Mechanism of boron removal

Figure 4 shows the morphology of impurities phases in the Al–30%Si alloy after Ar–H₂ gas blowing treatment. The photomicrograph of impurity phases and the corresponding EDS analysis results of different areas are illustrated in Fig. 4(a) and listed in Table 1, many coarse needle-like primary Si particles are distributed in the entire alloy and the average length of the primary Si is more than 10 μm. Two types of impurity phases were detected in the solidified Al–30%Si alloy, as shown in Fig. 4(a).

The difference in the color of the intermetallic phases is ascribed to the diverse composition and content of impurities. A grey suborbicular impurity phase (1#) is adhered to the boundary of needle-like primary Si particles with a diameter of 3 μm. As can be seen from Figs. 4(b) and (c), the main elements in 1# phase are B, Al, Ti and V, without Fe. The mole fraction of boron is 61.13% in the impurity phase, and the total mole fraction of Al and Ti is more than 27%. The possible existing compound is TiAl₃, TiB₂, AlB₂ or Al_x–Si_(1-x)–Ti ternary phase. According to Ref. [20], Ti only distributes at location where there is boron element in the grain centre of the primary silicon for Al–Si alloy within the addition of Al–Ti–B alloy. Where there is no boron element there is no Ti element, which indicates that the Ti-containing compound is TiB₂, not TiAl₃. In Ref. [21], TiB₂ solubility in molten Al was found to be rather small with a large temperature dependence. Moreover, TiAl₃ compound is found to be unstable in Al–Si alloy and

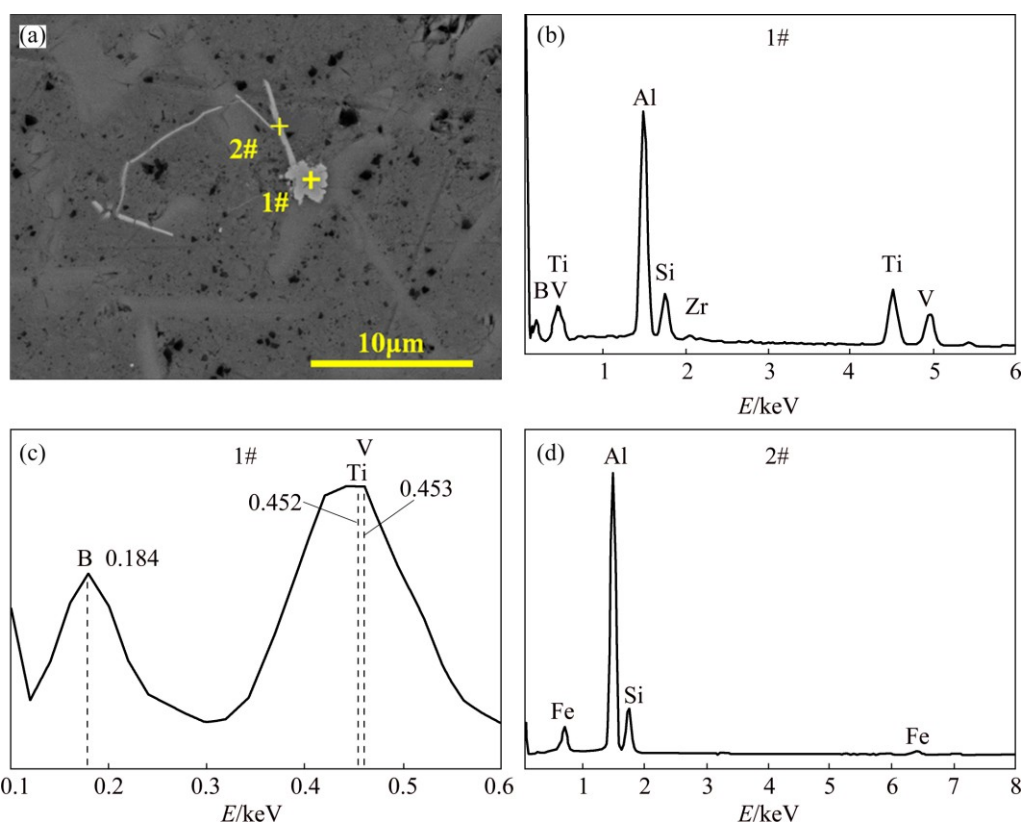


Fig. 4 Morphology (a) of impurity phases in solidified Al–30%Si alloy and corresponding EDS analyses (b–d)

Table 1 EDS quantitative analysis and chemical composition of impurity phases

| Sample | Mole fraction/% | | | | | | | Composition of phase |
|--------|-----------------|-------|-------|-------|------|------|-------|--|
| | B | Al | Si | Ti | V | Zr | Fe | |
| 1# | 61.13 | 14.02 | 3.3 | 13.13 | 8.04 | 0.38 | | TiB ₂ , AlB ₂ , VB |
| 2# | | 69.88 | 15.96 | | | | 14.15 | Al ₅ FeSi |

reacts with Si to form Ti–Si–Al compound and distributes in the matrix [22]. However, mole fraction of Si in the impurity phase is only 3.3%, few Ti–Si–Al ternary compounds exist in the impurity phases. Thus, the main phase (1#) in Fig. 4(a) can be regarded as TiB₂ and AlB₂.

As for TiB₂, the mole ratio of Ti to B is 1:2, and the mole ratio of Al to B is the same as 1:2 for AlB₂. According to the mass conversation, the mole ratio of boron to (Ti+Al) is 2:1 for TiB₂ and AlB₂. However, in this impurity phase, the mole ratio of boron to (Ti+Al) is larger than 2:1. The remained boron combines with V to form VB based on the mole ratio in the impurity phase (1#). By enlarging the EDS map shown in Fig. 4(c), the peak of boron in the EDS spectral line is 0.184 keV, and peaks of Ti and V are 0.452 and 0.453 keV, respectively. Ti and V have similar spectral line, which makes them have similar property, and thus, form the TiB₂ or VB

compound. From the perspective of thermodynamic, the Gibbs free energies of formation of TiB₂, VB and AlB₂ (Fig. 5) are –132.12, –131.10 and –71.65 kJ/mol at 973 K respectively as calculated by the software of HSC Chemistry. The Gibbs free energy of TiB₂ is also close to that of VB, and both of them are below zero. Hence, TiB₂ and VB are significantly more stable than AlB₂, which is consistent with Fig. 4(c). This indicates that TiB₂ and VB can be preferred to form. Therefore, the main impurity phases (1#) are TiB₂, AlB₂ and VB compounds.

At the same time, another light gray impurity phase is in long needle-like shape, which is shown in Fig. 4(a) (2#). EDS spectrum indicates that it only contains Al, Si and Fe, as shown in Fig. 4(d). It is clear from Table 1 that the needle-like phase (2#) contains about 69.88% Al, 15.96% Si and 14.15% Fe. From Refs. [18–21], the ternary intermetallic phases in Al–Si–Fe system are mainly α -Al₈SiFe₂, β -Al₅FeSi, γ -Al₃FeSi and δ -Al₄FeSi₂. Compared with other ternary phases, β -Al₅FeSi has the needle-like shape [22,23]. According to the mass fraction of each element, it can be concluded that the Al–Si–Fe impurity phase is β -Al₅FeSi intermetallic with the needle-like shape.

As for the removal mechanism of boron during Al–Si melt gas blowing, the explanation of that is shown as follows.

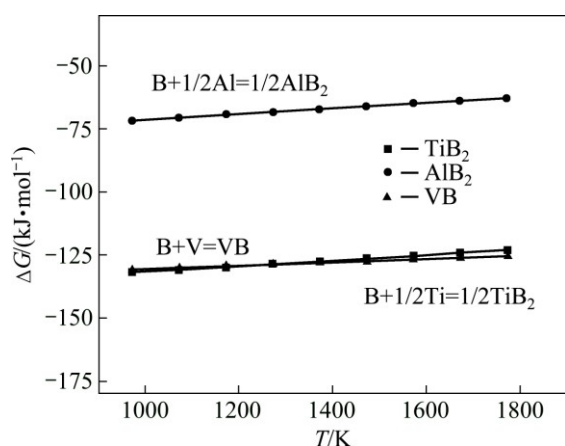


Fig. 5 Comparison of Gibbs free energy of TiB_2 , VB and AlB_2

It is well known that TiB_2 has hexagonal lattice structure with lattice parameters: $a=0.303$ nm, $b=0.303$ nm, $c=0.323$ nm, and its crystal structure is illustrated in Fig. 6(b). $\beta\text{-Al}_3\text{FeSi}$ phase is monoclinic structure [24]. But the crystal structure of Si is cubic with the lattice parameter: $a=0.357$ nm, which is shown in Fig. 6(a). Because the difference of crystal structure between Si and the impurity phases, the impurity elements segregated into the Al–Si eutectic from the primary Si in the form of impurity phase, especially as TiB_2 and VB. Considering the transformation of impurity phase in Fig. 3, it can be concluded that boron could be effectively removed by the segregation of TiB_2 and VB during Al–Si melt gas blowing treatment.

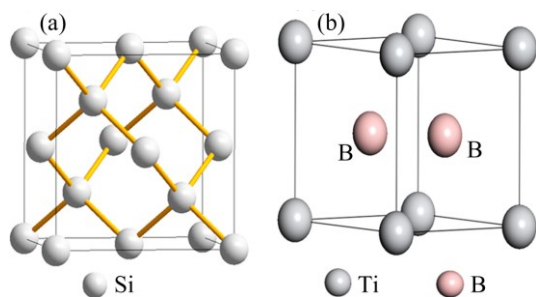


Fig. 6 Crystal structures of Si (a) and TiB_2 (b)

When H_2 is used as reaction gas, part of H_2 is dissolved in the Al–Si melt. The schematic drawing of boron removal is illustrated in Fig. 7. In Ref. [25], the effect of hydrogen content in the Ar– H_2 mixture about pure Si melt has been investigated. But little work has been focused on the Al–Si melt during gas blowing. This result reveals that H_2 addition increases the removal rate of boron significantly. The hydrogen in the Al–Si melt can be expressed as $[\text{H}]$ [16]. The $[\text{H}]$ reacts with the impurity $[\text{B}]$ in the molten Al–Si melt to form BH or BH_2 that has high vapour pressure, which can be taken out from the molten Al–Si melt within Ar– H_2 bubble.

From the perspective of purification, the Al–Si solvent refining principle is that the impurities in the MG–Si are segregated into the Al–Si melt, obtaining the high purity primary Si phases [8]. Thus, the segregation of the impurities occurs on the surface of the primary Si as shown in Fig. 2(a). If the number and the interface of the primary Si nucleation particles increase, the segregation efficiency could be improved. It is considered that the electromagnetic stirring used in the induction furnace can speed the diffusion of the B_xH_y (BH, BH_2) and B_xM_y (TiB_2 , VB and AlB_2) towards the interface of the primary Si or Al–Si melt.

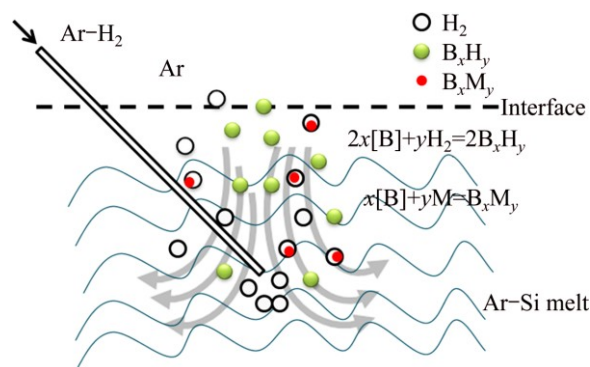


Fig. 7 Schematic drawing of boron by gas blowing treatment

4 Conclusions

- 1) Boron can be effectively removed from MG–Si using Ar– H_2 gas blowing technique during the Al–Si solvent refining. Compared with the sample without gas blowing, the removal efficiency of boron increases from 45.83% to 74.73% after 2.5 h.
- 2) Ar– H_2 blowing can refine the grain size and increase the nucleation of the primary Si. After 3.5 h Ar– H_2 blowing treatment, the average length of the primary Si in the alloy is shorter than that without gas blowing and many holes uniformly distribute in the Al–Si alloy after furnace cooling.
- 3) The main boron-containing impurity phase is in the form of TiB_2 , AlB_2 and VB compounds and the iron-containing phase is in the form of $\beta\text{-Al}_3\text{FeSi}$ intermetallic. They segregate into the Al–Si melt from the primary Si during the purification process. Part of boron transforms into gas B_xH_y (BH, BH_2) and diffuses towards the surface of volatilization by Ar– H_2 gas blowing treatment under electromagnetic stirring.

References

- [1] PIZZINI S. Towards solar grade silicon: Challenges and benefits for low cost photovoltaics [J]. Solar Energy Materials & Solar Cells, 2010, 94: 1528–1533.
- [2] TEIXEIRA L A V, TOKUDA Y, YOKO T, MORITA K. Behavior and state of boron in CaO-SiO_2 slags during refining of solar grade

- silicon [J]. ISIJ International, 2009, 49: 777–782.
- [3] ALEMANY C, TRASSY C, PATEYRON B, LIB K I, DELANNOY Y. Refining of metallurgical-grade silicon by inductive plasma [J]. Solar Energy Materials & Solar Cells, 2002, 72: 41–48.
- [4] HU Lei, WANG Zhi, GONG Xu-zhong, GUO Zhan-cheng, ZHANG Hu. Impurities removal from metallurgical-grade silicon by combined Sn–Si and Al–Si refining processes [J]. Metallurgical and Materials Transactions B, 2013, 44: 828–836.
- [5] HOFSTETTER J, LELIÈVRE J F, del CAÑIZO C, LUQUE A. Acceptable contamination levels in solar grade silicon: From feedstock to solar cell [J]. Materials Science and Engineering B, 2009, 159–160: 299–304.
- [6] YOSHIKAWA T, MORITA K. Refining of silicon during its solidification from a Si–Al melt [J]. Journal of Crystal Growth, 2009, 311: 776–779.
- [7] LI Jing-wei, GUO Zhan-cheng, TANG Hui-qing, LI Jun-cheng. Removal of impurities from metallurgical grade silicon by liquation refining method [J]. High Temperature Materials and Processes, 2013, 32: 503–510.
- [8] LI Jing-wei, GUO Zhan-cheng. Thermodynamic evaluation of segregation behaviors of metallic impurities in metallurgical grade silicon during Al–Si solvent refining process [J]. Journal of Crystal Growth, 2014, 394: 18–23.
- [9] TANG Kai, ØVRELID E J, TRANELL G, TANGSTAD M. A thermochemical database for the solar cell silicon materials [J]. Materials Transactions, 2009, 50: 1978–1984.
- [10] YU Wen-zhou, MA Wen-hui, LÜ Guo-qiang, REN Yong-sheng, XUE Hai-yang, DAI Yong-nian. Si purification by enrichment of primary Si in Al–Si melt [J]. Transactions of Nonferrous Metals Society of China, 2013, 23(11): 3476–3481.
- [11] LI Jing-wei, GUO Zhan-cheng, TANG Hui-qing, WANG Zhi, SUN Shi-tong. Si purification by solidification of Al–Si melt with super gravity [J]. Transactions of Nonferrous Metals Society of China, 2012, 22(4): 958–963.
- [12] LI Yan-lei, BAN Bo-yuan, LI Jing-wei, ZHANG Tao-tao, BAI Xiao-long, CHEN Jian, DAI Song-yuan. Effect of cooling rate on phosphorus removal during Al–Si solvent refining [J]. Metallurgical and Materials Transactions B, 2015, 46: 542–544.
- [13] LI Yan-lei, CHEN Jian, BAN Bo-yuan, ZHANG Tao-tao, DAI Song-yuan. Effect of cooling rate on boron removal and solidification behavior of Al–Si alloy [J]. High Temperature Materials and Processes, 2015, 34: 43–49.
- [14] LI Jia-yan, LIU Yao, TAN Yi, LI Ya-qiong, ZHANG Lei, WU Shen-rui, JIA Peng-jun. Effect of tin addition on primary silicon recovery in Si–Al melt during solidification refining of silicon [J]. Journal of Crystal Growth, 2013, 371: 1–6.
- [15] XU Fu-min, WU Shen-rui, TAN Yi, LI Jia-yan, LI Ya-qiong, LIU Yao. Boron removal from metallurgical silicon using Si–Al–Sn ternary alloy [J]. Separation Science and Technology, 2014, 49: 305–310.
- [16] LI Feng, XING Peng-fei, LI Da-gang, ZHUANG Yan-xin, TU Gan-feng. Removal of phosphorus from metallurgical grade silicon by Ar–H₂O gas mixtures [J]. Transactions of Nonferrous Metals Society of China, 2013, 23(11): 3470–3475.
- [17] WU Ji-jun, MA Wen-hui, LI Yan-long, YANG Bin, LIU Da-chun, DAI Yong-nian. Thermodynamic behavior and morphology of impurities in metallurgical grade silicon in process of O₂ blowing [J]. Transactions of Nonferrous Metals Society of China, 2013, 23: 260–265.
- [18] YOSHIKAWA T, MORITA K. Refining of silicon by the solidification of Si–Al melt with electromagnetic force [J]. ISIJ International, 2005, 45: 967–971.
- [19] YOSHIKAWA T, ARIMURA K, MORITA K. Boron removal by titanium addition in solidification refining of silicon with Si–Al melt [J]. Metallurgical and Materials Transactions B, 2005, 36: 837–842.
- [20] TANAHASHI M, FUJISAWA T, YAMAUCHI C. Oxidative removal of boron from molten silicon by CaO-based flux treatment with oxygen gas injection [J]. Metallurgical and Materials Transactions B, 2014, 45: 629–642.
- [21] YOSHIKAWA T, MORITA K. Thermodynamics of titanium and boron in molten aluminum [J]. Journal of The Japan Institute of Metals, 2004, 68: 390–394.
- [22] LIU L, SAMUEL A M, SAMUEL F H, DOTY H W, VALTIERRA S. Role of iron in relation to silicon modification in Sr-treated 319 and 356 alloys [J]. International Journal of Cast Metals Research, 2003, 16: 397–408.
- [23] ESFAHANI S, BARATI M. Purification of metallurgical silicon using iron as an impurity getter. Part I: Growth and separation of Si [J]. Metals and Materials International, 2011, 17: 823–829.
- [24] BATTEZZATI L, GREER A L. The viscosity of liquid-metals and alloys [J]. Acta Metallurgica, 1989, 37: 1791–1802.
- [25] NORDSTRAND E F, TANGSTAD M. Removal of boron from silicon by moist hydrogen gas [J]. Metallurgical and Materials Transactions B, 2012, 43: 814–822.

Ar–H₂ 混合气体对硅铝合金熔体精炼除硼机制的影响

李京伟, 白泉龙, 班伯源, 何秋湘, 陈健

中国科学院 应用技术研究, 新型薄膜太阳能电池重点实验室, 合肥 230031

摘要: 提出了一种将硅铝合金化与吹气精炼复合提纯冶金级硅的方法。在合金熔体 Ar–H₂ 吹气精炼过程中, 对硅中杂质相, 尤其是硼和铁的形态及转变进行了分析和表征, 并对除硼机制进行了讨论。实验结果表明: 合金吹气(Ar–H₂)精炼可以有效去除硅中的硼元素, 细化初晶硅颗粒和增加形核点的数量, 这有利于杂质元素的扩散转移。与未通气合金样品相比, 经过 2.5 h 吹气精炼, 硼的去除率由 45.83% 提高到 74.73%。含硼杂质相主要是 TiB₂、AlB₂ 和 VB 金属间化合物, 含铁杂质相主要是 β-Al₃FeSi 金属间化合物。同时, 硅中部分硼与溶解的[H]结合以 B_xH_y (BH, BH₂)形式在电磁搅拌作用下, 由合金熔体内部扩散到表面挥发, 达到除硼的目的。

关键词: 冶金级硅; 硅铝熔体; 吹气精炼; 除硼

(Edited by Xiang-qun LI)